

This article was downloaded by:

On: 25 January 2011

Access details: *Access Details: Free Access*

Publisher *Taylor & Francis*

Informa Ltd Registered in England and Wales Registered Number: 1072954 Registered office: Mortimer House, 37-41 Mortimer Street, London W1T 3JH, UK



Separation Science and Technology

Publication details, including instructions for authors and subscription information:

<http://www.informaworld.com/smpp/title~content=t713708471>

ADSORPTION AND STEAM REGENERATION OF n-HEXANE, MEK, AND TOLUENE ON ACTIVATED CARBON FIBER

Jong-Hwa Kim^a; Yong-Ki Ryu^a; Seungjoo Haam^a; Chang-Ha Lee^a; Woo-Sik Kim^a

^a Department of Chemical Engineering, Yonsei University, Seoul, South Korea

Online publication date: 03 December 2001

To cite this Article Kim, Jong-Hwa , Ryu, Yong-Ki , Haam, Seungjoo , Lee, Chang-Ha and Kim, Woo-Sik(2001) 'ADSORPTION AND STEAM REGENERATION OF n-HEXANE, MEK, AND TOLUENE ON ACTIVATED CARBON FIBER', *Separation Science and Technology*, 36: 2, 263 – 281

To link to this Article: DOI: 10.1081/SS-100001078

URL: <http://dx.doi.org/10.1081/SS-100001078>

PLEASE SCROLL DOWN FOR ARTICLE

Full terms and conditions of use: <http://www.informaworld.com/terms-and-conditions-of-access.pdf>

This article may be used for research, teaching and private study purposes. Any substantial or systematic reproduction, re-distribution, re-selling, loan or sub-licensing, systematic supply or distribution in any form to anyone is expressly forbidden.

The publisher does not give any warranty express or implied or make any representation that the contents will be complete or accurate or up to date. The accuracy of any instructions, formulae and drug doses should be independently verified with primary sources. The publisher shall not be liable for any loss, actions, claims, proceedings, demand or costs or damages whatsoever or howsoever caused arising directly or indirectly in connection with or arising out of the use of this material.

ADSORPTION AND STEAM REGENERATION OF n-HEXANE, MEK, AND TOLUENE ON ACTIVATED CARBON FIBER

Jong-Hwa Kim, Yong-Ki Ryu, Seungjoo Haam,
Chang-Ha Lee,* and Woo-Sik Kim

Department of Chemical Engineering, Yonsei University,
Shinchon-dong, Seodaemun-gu, Seoul, 120-749,
South Korea

ABSTRACT

The adsorption and steam regeneration of n-hexane, MEK, and toluene on an activated carbon fiber (ACF) were conducted for single, binary, and ternary systems and were compared with those on a granular activated carbon (GAC). An ACF bed showed not only larger adsorption capacity but also faster steam regeneration than the GAC bed. Also, the tailing effect of desorption on a GAC loaded with polar MEK was significant compared with the result on an ACF. Especially, after several adsorption-desorption cycles, there was a significant drop in the adsorption capacity of the GAC within 20% whereas the adsorption capacity of the ACF dropped within 5%. Because adsorption affinity on the ACF became stronger for toluene, MEK, and n-hexane in sequence, roll-up phenomena appeared for binary and ternary systems. Because the roll-up phenomenon was affected by the molar ratio (MR), the magnitude of

*Corresponding author. E-mail: leech@yonsei.ac.kr

roll-up increased with a decrease of MR. Therefore, the adsorption step in a TSA process could be determined largely by the behavior of a weak adsorbate in the adsorption bed, whereas a strong adsorbate could play a key role in the steam regeneration step. However, under a high MR, both the high concentration component and strongest adsorbed component played an important role in steam regeneration.

Key Words: Adsorption; Steam regeneration; ACF; MR; Roll-up

INTRODUCTION

Volatile organic compounds (VOCs) are among the most common pollutants emitted by chemical process industries (CPI). Accordingly, VOC emission control is a major portion of the CPI's environmental activities (1). VOCs cause ground level ozone through photochemical reaction and have been one of the major causes of air pollution. VOCs are usually discharged in the air at a gas phase due to their strong volatility and directly affect a laborer's health as well as air pollution. Current maximum achievable control technologies for VOCs are condensation, incineration, adsorption, and absorption. Of these technologies, the adsorption process is more common, offering some advantages over the others (2). This process is cost effective because it is a proven and reliable pollution control technology that has the added benefit of recovering valuable materials for reuse (3). For many adsorption applications, both a granular activated carbon (GAC) and an activated carbon fiber (ACF) are used (4).

ACFs provide greater ease of use than GACs because the ACFs are not granules but can be manufactured in the form of cloth. Also, it has many favorable characteristics such as high adsorption capacity and high mass transfer rate for both adsorption and desorption. Because an ACF has a large specific surface area and a pore structure with less than 2 nm micropores, its diffusion path for adsorbates is short (5). Therefore, an ACF typically exhibits higher adsorption capacities and faster adsorption kinetics than a GAC.

When the GAC or ACF becomes exhausted or when the effluent from the bed reaches a maximum allowable discharged level, the spent GAC or ACF must be processed to remove the adsorbate, which regenerates the carbon for subsequent use again as an adsorbent. The regeneration process can be carried out by extraction using chemical regeneration or thermal treatments. Steam regeneration, one of the several regeneration methods, is the most widely used *in situ* method of GAC bed regeneration. Because of partial condensation and adsorption, steam with its high heat content can provide significantly more energy to desorb the solvent than hot inert gas does. Furthermore, adsorbed water competes with the



solvent for pore volume of the adsorbent to enhance desorption (7). However, although regeneration is the energy-intensive phase of an adsorption cycle, it is rarely the time limiting step. Some fundamental researches of either theoretical or experimental nature for steam regeneration in the GAC bed have been performed to improve our understanding of the process (6,7).

In this study, the adsorption and steam regeneration of MEK, toluene, and n-hexane on the adsorption bed packed with ACFs were investigated. The effects of feed concentration, temperature, and steam flow rate were studied and the results in the ACF bed were compared with those in the GAC bed. To understand the effect of polarity and adsorption affinity, the adsorption and steam regeneration experiments have been carried out for single, binary, and ternary systems. It is desirable to have a basic understanding of the mechanisms controlling adsorption and steam regeneration of VOCs in the ACF bed as a basis for designing reliable and efficient adsorption process based separation devices. Therefore, the ultimate goal of this work is to establish a feasible recovery system of VOCs in the ACF adsorption process by steam regeneration.

MATERIALS AND EXPERIMENTAL METHODS

MEK (Reagent grade, Tedia, USA), toluene (HPLC grade, Aldrich, USA), and n-hexane (HPLC grade, Sigma-Aldrich, USA) were selected as adsorbates. VOC concentrations in the range of 0.078–0.708 mol/m³ were tested. As adsorbents, a GAC (GURACOAL-GW, Kuraray Co., Japan) of uniform size obtained by sieving and a felt-type cellulose-based ACF (KF-1500, Toyobo Co., Japan) were used in this study. The ACF and GAC were boiled in deionized and ultrafiltered water to remove fines. To eliminate any trace of pollutants, the ACF and GAC were kept in a drying oven for 24 h at 448 K. The results of the BET analysis showed that only micropores (less than 20 Å) were well developed in the ACF and micropores and mesopores (20–500 Å) coexisted in the GAC. The physical properties of the ACF and GAC are listed in Table 1.

To determine dynamic behavior during adsorption and steam regeneration, experimental adsorption and desorption curves were collected under various

Table 1. Properties of Adsorbents

Property	GAC	ACF
Approximate shape	Sphere	Cylinder
Average particle diameter	425 μm	17.5 μm
Specific surface area	1200–1300 m ² /g	1440–1450 m ² /g
Average micropore diameter	<20 Å	<20 Å



loading and steam conditions. The schematic diagrams of the fixed bed apparatus are presented in Figure 1.

The adsorption column used in this study was made of a stainless steel tube with an inside diameter of 1.27 cm. The length of the bed packed with the same amount of pretreated ACF and GAC, respectively, was less than 4 cm to prevent the steam condensation in the bed. In addition, glass wool was packed on both ends of the bed to prevent the carryover of adsorbent and the end effect. After packing the prepared carbon in the bed, the system was filled with N₂ at 1 atm to prevent surrounding air contact. Temperature in the bed was measured with a K-type thermocouple located at the bottom of the adsorbent through the bed. Additional thermocouples were installed in the feed or steam line to measure the inlet temperature. To prevent condensation, all lines carrying steam or feed vapors were heat-traced using electrical heating tapes, and the bed was insulated by glass fiber.

Flows in the bed were upward for the adsorption experiment and downward for steam regeneration. The feed flow rate from a VOC generator was measured with a rotameter that was precalibrated against a wet gas meter. The system pressure was measured by pressure gauges, which were installed above and below the bed.

As shown in Figure 1, in order to provide a sufficient mixing time and prevent condensation, a 20-liter mixing chamber was installed at the inlet of the adsorption bed with a temperature of 298 K using an electrical heater. In the adsorption experiments, the inlet concentrations of VOCs were adjusted by diluting VOCs generated from the generator with nitrogen in the mixing chamber. The feed was vented until its concentration was constantly maintained at the desired value. To prevent the change of feed concentration from a pressure drop, the identical adsorption bed was equipped with a vent line. Then, this concentration was identified several times by a GC with a flame ionization detector (FID) before feeding the adsorption bed. The concentration of column effluent was collected at the sampling port and was measured by the GC. The experiment was terminated when the effluent concentration of VOCs became equal to the imposed concentration at the inlet.

The saturated column previously used for breakthrough experiment was applied for steam regeneration. After generating 373 K steam at a preheater, the desired steam temperature was controlled by a steam generator. The steam temperatures were measured by the K-type thermocouples installed in the top of the bed and the bottom of the adsorbent inside the bed. After the generated steam reached the desired temperature and flow rate, the steam was used for the regeneration of the bed. The steam flow rate from an electric steam generator was set with a metering valve and measured with a balance by condensing the steam through the condenser. Desorbed adsorbates by steam were condensed and collected in a vial bottle filled with CS₂. Then, desorbed amounts of adsorbates were measured by the GC periodically. After removing moisture in the column at a drying oven, the



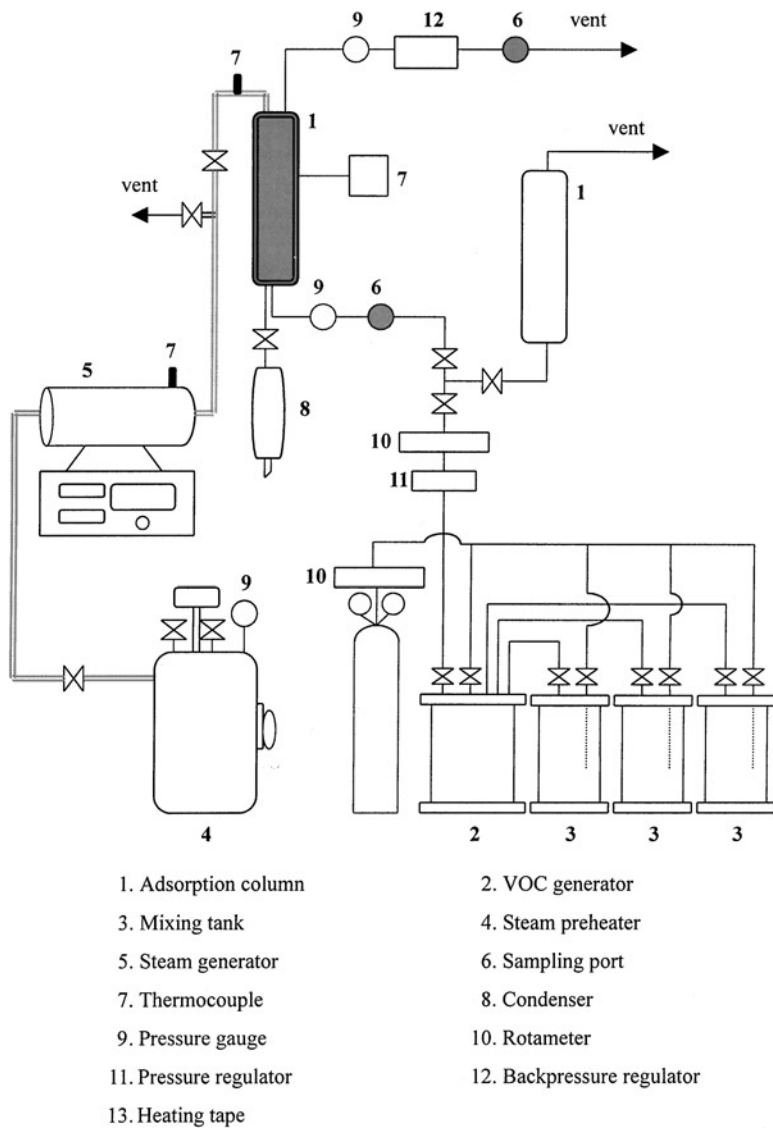


Figure 1. Schematic diagram of experimental adsorption and steam regeneration apparatus.



adsorption capacity of regenerated adsorbents was tested through breakthrough experiments.

RESULT AND DISCUSSION

Comparison of Adsorption Capacity between Regenerated ACF and GAC

Figure 2 shows the comparison of the adsorption capacity between the regenerated ACF and GAC. After the adsorption experiment, the ACF and GAC loaded with MEK were regenerated by steam at 393 K. As shown in Figure 2a, there was approximately a 5% drop in the adsorption capacity of the ACF after three cycles of regeneration. However, the difference in the adsorption capacity between the third regeneration and the fourth regeneration was very small. In the case of the GAC, the adsorption capacity dropped by 20% after the fourth regeneration showed a significant decrease of adsorption capacity in the first regeneration. This significant drop in the adsorption capacity of the GAC can be explained by irreversible chemisorption. It is well known that there are more various functional groups in the GAC surface than in the ACF surface, and chemisorption by interaction between adsorbates and functional groups may occur (16,17). Moreover, the breakthrough time of the fourth regenerated ACF bed packed with 0.6 g adsorbents was longer than that of the third regenerated GAC bed packed even with 1.0 g adsorbents. Also, in all cases, the breakthrough curves at the ACF bed were much steeper than those at the GAC bed. Therefore, it implies that the ACF can be more efficiently used for treatment and recovery of VOCs in terms of adsorption capacity.

Adsorption and Desorption of Single Component System

The effect of bed temperature on the breakthrough curves of MEK and n-hexane was experimented. In Figure 3, because it was very difficult to make the exact same concentration for each adsorbate run by the saturating generation system, the feed concentration was slightly different at each run. As shown in Figure 3, the adsorption capacity increases almost proportionally with a decrease of temperature because physical adsorption is an exothermic process. However, the breakthrough time of each curve is not much different in the experimental range of temperature.

Experimental breakthrough curves for pure components on the ACF and GAC are shown in Figure 4. The degree of separation depends on the sharpness of the concentration wave front, also referred to as the mass transfer zone. The sharpness of the concentration front is measured by the breakthrough curve (8). As



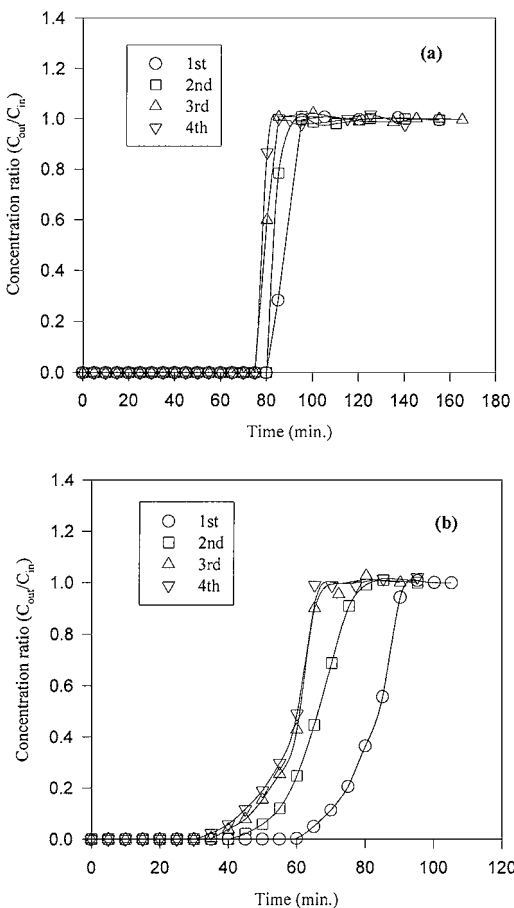


Figure 2. Breakthrough curves of MEK on regenerated a) ACF and b) GAC. a) ACF: 0.600 g, C_{in} : 0.484 gmol/m³, Flow rate: 49 ml/min. b) GAC: 0.600 g, C_{in} : 0.487 gmol/m³, Flow rate: 48 ml/min.

shown in Figure 4, the lower the feed concentration, the longer the breakthrough time in the ACF bed. Also, the breakthrough curves for all three adsorbates in the ACF bed were steeper than those in the GAC bed. This is because adsorbates in an ACF with only micropores reach adsorption sites through micropores without the additional diffusion resistance of mesopores, unlike a GAC. Therefore, the ACF provided faster adsorption and narrower mass transfer zone compared to the GAC.

When the adsorption amount of each pure adsorbate in both the ACF and GAC was calculated from the breakthrough curve, the adsorption amount of toluene in the ACF was about 62% higher than that in the GAC. However, the adsorption



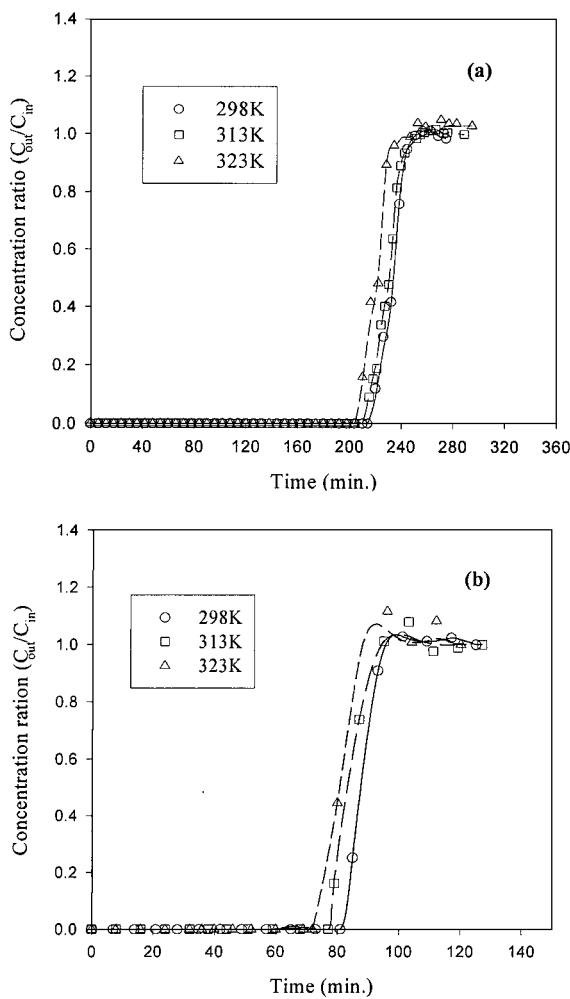


Figure 3. Breakthrough curves of a) MEK and b) n-hexane in ACF bed at 298 K.
 a) Adsorbent: 0.600 g, C_{in} : 0.147 gmol/m³, Flow rate: 40 ml/min. b) Adsorbent: 0.602 g, C_{in} : 0.323 gmol/m³, Flow rate: 40 ml/min.

amount of MEK in the ACF was about 15% higher than that in the GAC. In the case of n-hexane, the adsorption amount in ACF was slightly higher than that in the GAC. Especially, in spite of the lower molecular weight and feed concentration of MEK, the breakthrough time of MEK in both the ACF and GAC was longer than that of n-hexane due to a polarity of MEK. Therefore, the higher the adsorption



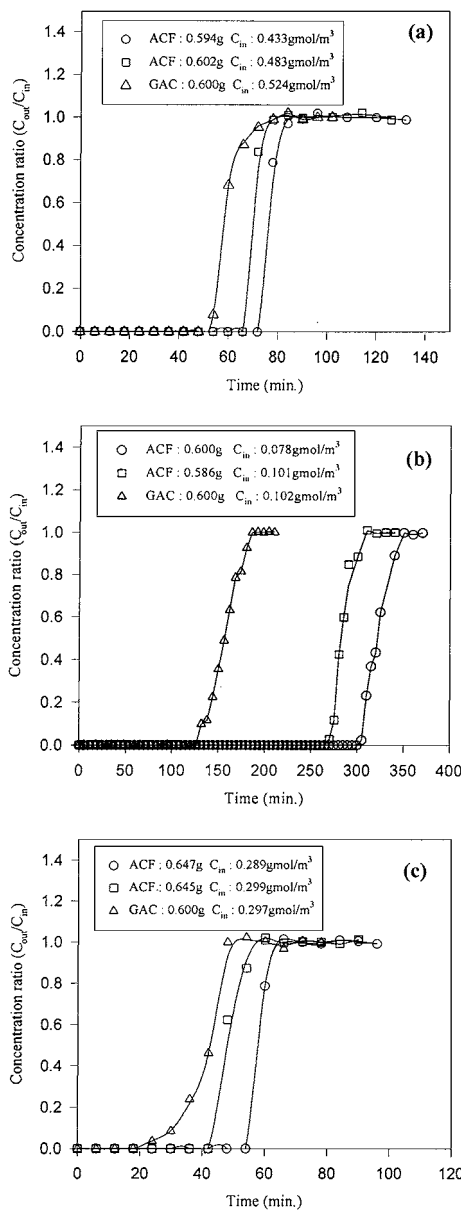


Figure 4. Breakthrough curves of a) MEK, b) toluene, and c) n-hexane at 298 K. (Flow rate: a) 63 ml/min, b) 60 ml/min, c) 65 ml/min.)



affinity, the larger the difference in the adsorption capacity between the ACF and GAC.

The results of steam regeneration of the adsorption bed adsorbed by a single component are shown in Figure 5. The desorption time was lengthened in the sequence of adsorption affinity. And the dip phenomenon of the desorption curve (13,14) was not observed due to the high heat capacity of steam. Because the hot steam lost its energy by the cold bed and strong endothermic processes, the desorption rate at the beginning period of regeneration was affected by a steam flow rate in Figure 5. However, the complete desorption time in the ACF bed was almost the same regardless of steam flow rate due to the heat transfer by steam with the high heat capacity. The desorption of the VOC was faster in the ACF bed than in the GAC bed due to the ACF's unique pore structure. In all three cases, the tailing effect was more significant at the GAC bed than at the ACF bed.

In Figure 5a, the polar MEK in the saturated GAC bed was desorbed very well by steam at the initial interval. However, after a short period of time, the mass transfer zone of the desorption curve became very broad and showed a large tail due to the high adsorption affinity on the surface of the activated carbon. The regeneration of the ACF adsorbed by toluene in Figure 5b was almost completed within 20 min like the result of MEK in Figure 5a even though the regeneration rate of the ACF at the beginning period was slower than that adsorbed by MEK. However, the toluene on the GAC bed was desorbed steadily by steam showing the shorter desorption tail than that of MEK even though the desorption rate of toluene was slower than that of MEK due to the strong adsorption. In Figure 5c, the desorption of a n-hexane made a little difference according to the steam flow rate and the adsorbent in comparison with the results of MEK and toluene, as n-hexane is a weak and nonpolar adsorbate. In the case of toluene and MEK, the tailing effect at the ACF bed even in the low steam rate became smaller than that at the GAC bed in high steam flow rate. Meanwhile, the difference between the desorption tails of n-hexane in both adsorbents was relatively very small.

From the result of steam regeneration of the adsorption bed adsorbed by a single component, more steam and higher energy are needed for the GAC bed than the ACF, which is adsorbed by n-hexane, MEK, and toluene to complete the regeneration. Therefore, in the case of these VOCs, ACF showed better characteristics for adsorption and steam regeneration than GAC.

Adsorption and Desorption of Binary System

The shapes of the mass transfer zone in breakthrough curves for a binary system were different from those for a single component system. The velocity of each concentration wavefront can be determined mainly by feed rates, feed



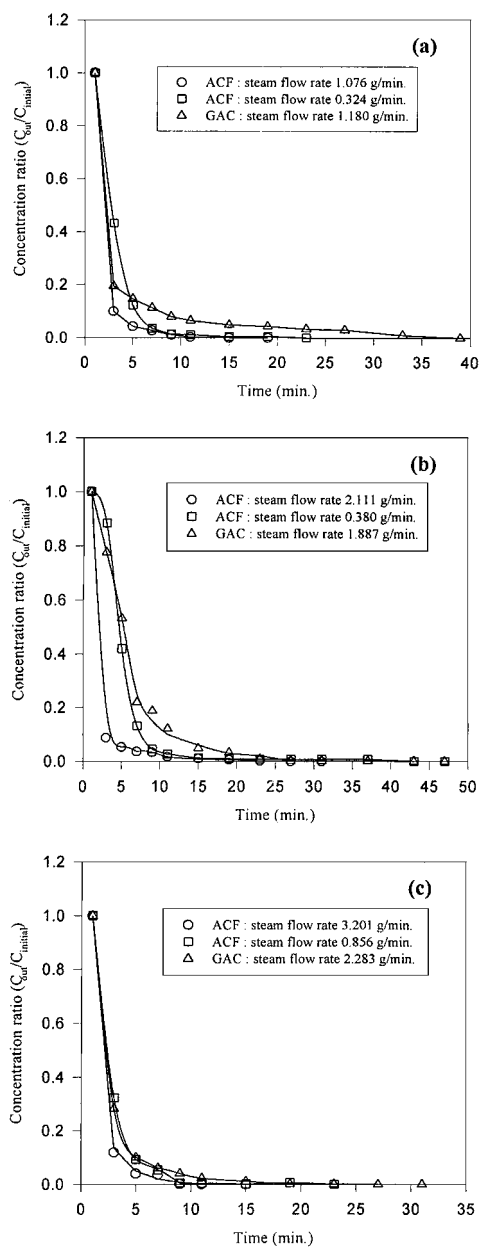


Figure 5. Desorption curve of a) MEK, b) toluene, and c) n-hexane at 393 K.



compositions, and adsorption capacities as revealed by the equilibrium theory (9). As shown in Figure 6, the roll-up of MEK in a MEK/toluene system was observed due to the strong adsorption of toluene. This roll-up phenomenon was also observed in n-hexane/toluene and n-hexane/MEK systems. The well-known roll-up phenomenon results from the fact that weakly adsorbed components lose their adsorption sites due to the competitive adsorption of more strongly adsorbed components that follow the preceding wavefronts of weakly adsorbed components (18). The desorbed adsorbates join the bulk stream and increase the concentration more than the feed concentration.

According to these binary breakthrough experiments, an adsorption affinity to an ACF was toluene, MEK, and n-hexane in sequence as expected in Figure 4. The roll-up phenomenon was affected by molar ratio (MR) defined as the ratio of the influent concentration of a weak adsorbent to the influent concentration of a strong adsorbent (10). It was found that the magnitude of roll-up was larger at a smaller MR as clearly shown in Figures 6b and c. Also, in MEK/toluene and n-hexane/toluene systems with a similar MR, the magnitude of roll-up by toluene was much higher in the n-hexane/toluene system than that in the MEK/toluene system. However, the breakthrough time of toluene was similar in these systems.

After the bed was saturated with a binary mixture, regeneration was started by using hot steam. As shown in Figure 7, the strong adsorbate played a key role in the steam regeneration of the ACF because a strong adsorbate was mostly adsorbed by displacing a weak adsorbate at the adsorption step. Also, the desorption of a strong adsorbate by steam showed a long tail. As shown in Figure 7a in the case of a high concentration of MEK in the toluene/MEK system, a certain amount of MEK was adsorbed even though MEK was rolled up by toluene in the adsorption step. However, in the n-hexane/toluene system in Figure 7b, only a fraction of n-hexane was left in the bed after the adsorption step although a higher concentration of n-hexane was fed to the adsorption bed. Similarly, because most of the bed was saturated with MEK in the n-hexane/MEK system, the regeneration time depended on the desorption of MEK in Figure 7c. Also, at less than a 1.1 g/min steam flow rate, the desorption of solvents in Figures 7a and c was hardly affected by the steam flow rate because the hot steam lost its energy by the cold bed and strong endothermic processes.

Adsorption and Desorption of Ternary System

As shown in Figure 8, n-hexane was the first breakthrough component followed by MEK at close intervals, and finally, the breakthrough of toluene occurred in the ACF bed. As expected in Figure 6, there was no big difference in magnitudes of roll-up for MEK and n-hexane at similar MR (MR = 1~2). After



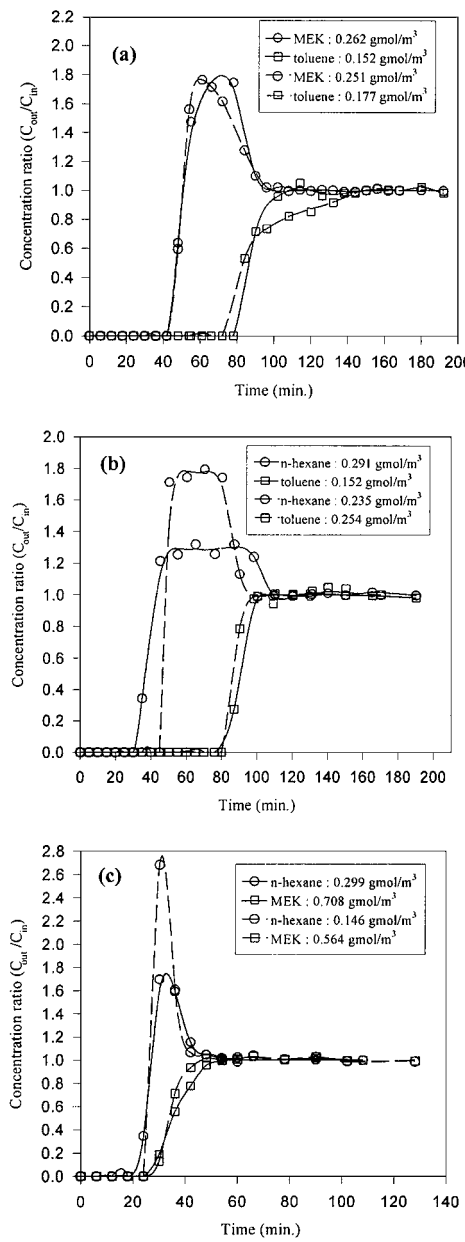


Figure 6. Breakthrough curve of a) MEK/toluene, b) n-hexane/toluene, and c) n-hexane/MEK system at 298 K. – : ACF amount (g), flow rate (ml/min.) a) 0.599, 68, b) 0.586, 51, c) 0.619, 64; ... : ACF amount (g), flow rate (ml/min.) a) 0.632, 70, b) 0.611, 48, c) 0.632, 68.



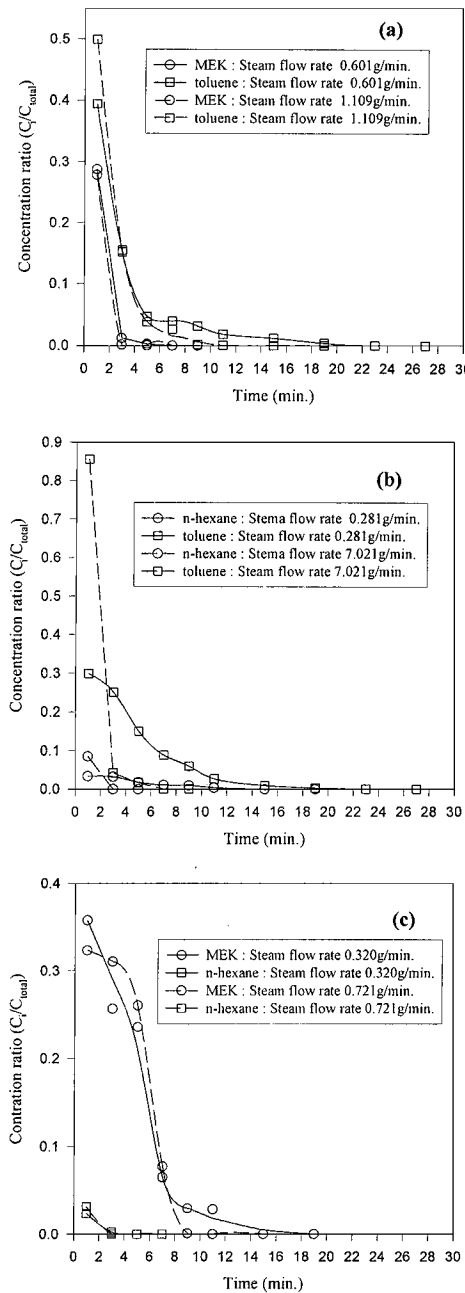


Figure 7. Desorption curve of a) MEK/toluene, b) n-hexane/toluene, and c) n-hexane/MEK system at 393 K steam temperature.



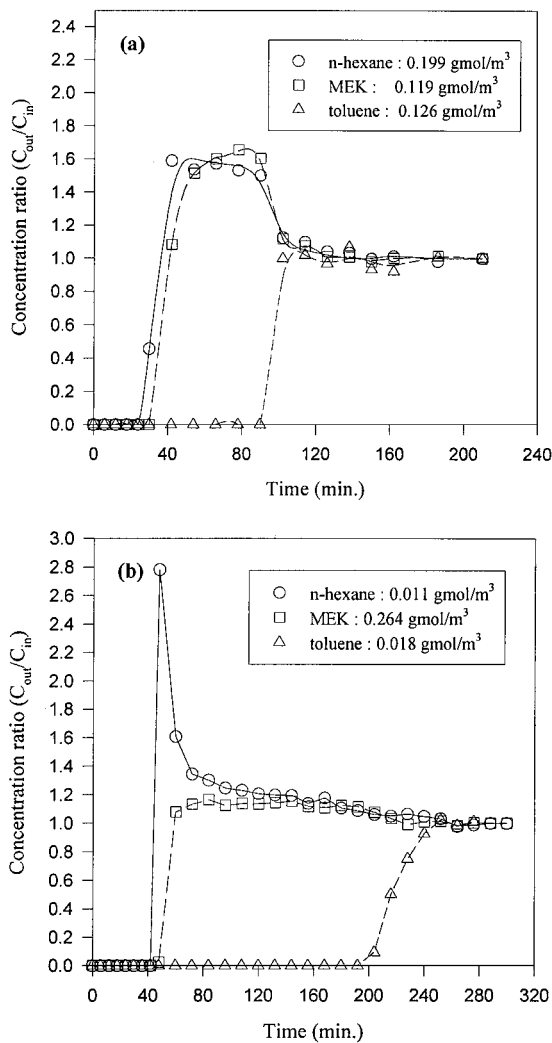


Figure 8. Breakthrough curve of MEK/toluene/n-hexane system under a) similar MR and b) different MR conditions at 298 K. a) Adsorbent: 0.600 g, C_{in} : 0.147 gmol/m³, Flow rate: 40 ml/min. b) Adsorbent: 0.602 g, C_{in} : 0.323 gmol/m³, Flow rate: 40 ml/min.

starting the breakthrough and roll-up of n-hexane, the breakthrough of MEK began at the highest point of the roll-up of n-hexane. Then, the roll-ups of both n-hexane and MEK decreased smoothly from the breakthrough point of toluene as shown in Figure 8a. At a different MR with a high concentration of MEK (MR for MEK/



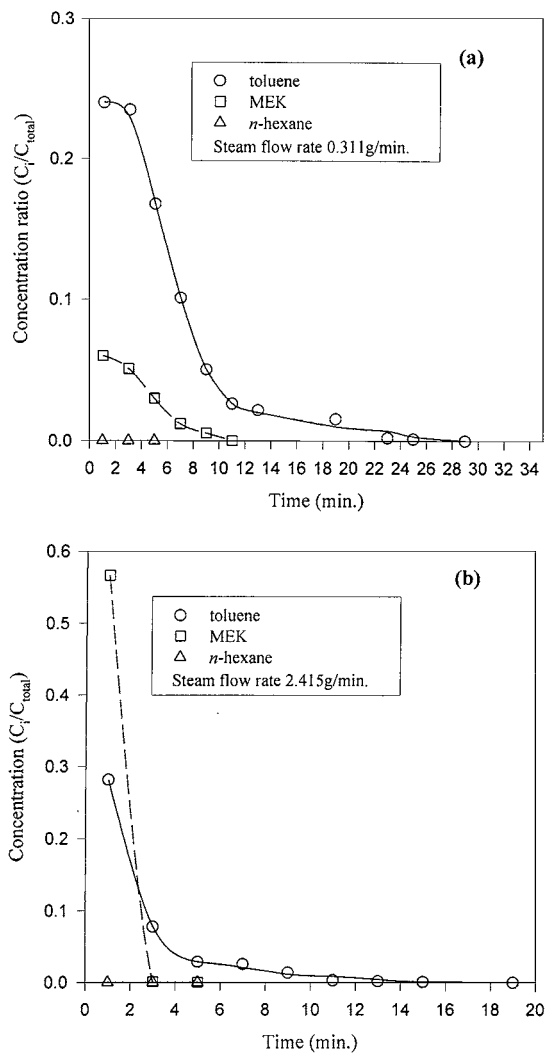


Figure 9. Desorption curve of toluene/MEK/*n*-hexane system under a) similar MR and b) different MR conditions at 393 K steam temperature.

toluene = 14.73, MR for *n*-hexane/MEK = 0.042), a significant roll-up of *n*-hexane was observed by a high concentration of MEK. However, the roll-up of MEK was not prominent in the ACF bed, as shown in Figure 8b. This wide but small roll-up of MEK showing a plateau results from the small amount of toluene in the feed. Also, the breakthrough time of toluene was elongated more than that in Figure 8a, due



to the low concentration of toluene. Therefore, the wavefront of toluene proceeds slowly and some preoccupying adsorbates, such as MEK and n-hexane, continue to diffuse out due to a competitive adsorption until the breakthrough of toluene occurs.

The bed saturated with a ternary mixture was regenerated by using hot steam. By displacing n-hexane by strong adsorbates in Figures 8a and b, n-hexane was hardly adsorbed in the ternary system, as shown in Figures 9a and b. In the case of an adsorption bed adsorbed by a similar MR condition in Figure 9a, only a fraction of MEK was left in the bed. And the adsorbed MEK was relatively desorbed within a short period of time, while the adsorbed toluene was desorbed with a long tail. However, in the case of a high concentration of MEK in the ternary system, as shown in Figure 9b, a certain amount of MEK was adsorbed. However, the adsorbed MEK was desorbed at the beginning of regeneration without a tail, and the desorption of toluene showed a long tail like Figure 9a. Therefore, under the experimental MR range in the ternary system, the adsorption step time could be determined largely by the behavior of n-hexane in the adsorption bed due to the early breakthrough and roll-up of n-hexane. Meanwhile, the toluene could play a key role in the steam regeneration step time because of the slow desorption and long tail.

CONCLUSIONS

The adsorption and steam regeneration of n-hexane, MEK, and toluene were investigated in a fixed bed packed with activated carbon fiber (ACF). The adsorption and desorption experiments of these solvent vapors on the ACF were conducted for single, binary, and ternary systems and compared with those on granular activated carbon (GAC).

In single component systems, due to the ACF's unique structure with only micropores and large surface area, the adsorption capacity of VOCs was higher at the ACF bed than at the GAC bed, and breakthrough curve was steeper at the ACF bed than at the GAC bed. The tailing effect of desorption on the GAC, especially loaded with polar MEK, was significant when compared with the result on the ACF. Also, after several adsorption-desorption cycles, the decrease of the adsorption capacity was much larger for the GAC than for the ACF. It implies that an ACF could be more efficiently used for VOC treatment than a GAC.

In this study, the adsorption affinity of toluene with the largest molecular weight on both adsorbents was stronger than that of the others. However, MEK, which is polar, showed stronger adsorption than n-hexane with a larger molecular weight. Therefore, the roll-up phenomena appeared for both binary and ternary systems. Because roll-up was affected by molar ratio (MR), the smaller MR made the larger roll-up. When the adsorption in the bed occurred under similar molar



ratio, the toluene was a key component in steam regeneration due to the roll-up phenomena of the weak adsorbates. However, in the case of a breakthrough under different molar ratio, both the high concentration component and strongest adsorbed component played an important role in steam regeneration.

ACKNOWLEDGMENT

This work was supported by KOSEF under project 95-0502-01-3.

SYMBOLS

C	adsorbate concentration in the bulk fluid phase [gmol/m ³]
C_i	component desorbed concentration [gmol/l]
C_{initial}	initially desorbed concentration [gmol/l]
C_{total}	total component desorbed concentration [gmol/l]
C_{01}	weakly adsorbed species [gmol/cm ³]
C_{02}	strongly adsorbed species [gmol/cm ³]
T	temperature

Subscripts

in	input adsorbate concentration [gmol/m ³]
out	output adsorbate concentration [gmol/m ³]
i	component number

REFERENCES

1. Ruddy, E.N.; Carroll, L.A. Select the Best VOC Control Stragy. *Chem. Eng. Prog.* **1993**, 89, 28.
2. Nirmalakhandan, N.N.; Speece, R.E. Prediction of Activated Carbon Adsorption Capacities for Organic Vapors Using Quantitative Structure Relationship Methods. *Environ. Sci. Technol.* **1993**, 27, 1512.
3. Ruhl, M.J. Recover VOCs via Adsorption on Activated Carbon. *Chem. Eng. Prog.* **1993**, 89, 37.
4. Lin, T.F.; Little, J.C.; Nazarof, W.W. Transport and Sorption of Organic Gases in Activated Carbon. *J. Environ. Eng.* **1996**, 122, 169.
5. Xiu, G.H. Modeling Breakthrough Curves in a Fixed Bed of Activated Carbon Fiber-Exact Solution and Parabolic Approximation. *Chem. Eng. Sci.* **1996**, 51, 4039.



6. Schwiger, T.A.J. A Design Method for Adsorption Bed Capacity: Steam-Regenerated Adsorbers. *Ind. Eng. Chem. Res.* **1996**, 35, 1929.
7. Schwiger, T.A.J.; LeVan, M.D. Steam Regeneration of Solvent Adsorbers. *Ind. Eng. Chem. Res.* **1993**, 32, 2418.
8. Cen, P.L.; Yang, R.T. Analytic Solution for Adsorber Breakthrough Curves with Bidisperse Sorbents (Zeolites). *AIChE J.* **1986**, 32, 1635.
9. Farooq, S.; Ruthven, D.M. Dynamics of Kinetically Controlled Binary Adsorption in a Fixed Bed. *AIChE J.* **1991**, 37, 299.
10. Noll, K.E.; Gounaris, V.; Hou, W.S. *Adsorption Technology*; Lewis Publishers: Michigan, 1992.
11. Chihara, K.; Suzuki, M. J. Simulation of Nonisothermal Pressure Swing Adsorption. *Chem. Eng. Jpn.* **1983**, 16, 53.
12. Schweiger, T.A.J. Effects of Water Residues on Solvent Adsorption Cycles. *Ind. Eng. Chem. Res.* **1995**, 34, 283.
13. Huang, C.C.; Fair, J.R. Study of the Adsorption and Desorption of Multiple Adsorbates in a Fixed Bed. *AIChE J.* **1988**, 34, 1861.
14. Huang, C.C.; Hwu, T.L.; Hsia, Y.S. Recovery of Aceton Vapor by a Thermal Swing Adsorber with Activated Carbon. *J. Chem. Eng. Jpn.* **1993**, 26, 21.
15. Schork, J.M.; Fair, J.R. *Ind. Eng. Chem. Res.* **1988**, 27, 1545.
16. Byeon, S.H.; Oh, S.M.; Kim, W.S.; Lee, C.-H. Evaluation of an Activated Carbon Felt Passive Sampler in Monitoring Organic Vapors. *Industrial Health* **1997**, 35, 404.
17. Lee, C.-H.; Yang, J.; Kim, C.W.; Cho, C.H.; Lee, H. *HWAHAK KONGHAK* **1997**, 35, 69.
18. Yang, J.; Lee, C.-H. Adsorption Dynamics of a Layered Bed PSA for H₂ Recovery from Coke Oven Gas. *AIChE J.* **1998**, 44, 1325.

Received October 8, 1999

Revised May 2000



Request Permission or Order Reprints Instantly!

Interested in copying and sharing this article? In most cases, U.S. Copyright Law requires that you get permission from the article's rightsholder before using copyrighted content.

All information and materials found in this article, including but not limited to text, trademarks, patents, logos, graphics and images (the "Materials"), are the copyrighted works and other forms of intellectual property of Marcel Dekker, Inc., or its licensors. All rights not expressly granted are reserved.

Get permission to lawfully reproduce and distribute the Materials or order reprints quickly and painlessly. Simply click on the "Request Permission/Reprints Here" link below and follow the instructions. Visit the [U.S. Copyright Office](#) for information on Fair Use limitations of U.S. copyright law. Please refer to The Association of American Publishers' (AAP) website for guidelines on [Fair Use in the Classroom](#).

The Materials are for your personal use only and cannot be reformatted, reposted, resold or distributed by electronic means or otherwise without permission from Marcel Dekker, Inc. Marcel Dekker, Inc. grants you the limited right to display the Materials only on your personal computer or personal wireless device, and to copy and download single copies of such Materials provided that any copyright, trademark or other notice appearing on such Materials is also retained by, displayed, copied or downloaded as part of the Materials and is not removed or obscured, and provided you do not edit, modify, alter or enhance the Materials. Please refer to our [Website User Agreement](#) for more details.

Order now!

Reprints of this article can also be ordered at
<http://www.dekker.com/servlet/product/DOI/101081SS100001078>